# Non-linear MHD Simulations of Pellet Triggered ELM for ITER Plasma Scenarios

S. Futatani[1,2], G.T.A. Huijsmans[3], A. Loarte[4], M. Mantsinen[1,5], S. Pamela[6], L. Garzotti[6], M. Hoelzl[7], P.T. Lang[7], F. Orain[7]
[1]*Barcelona Supercomputing Center (BSC), C/ Jordi Girona 29, 08034-Barcelona, Spain*
[2]*EUROfusion Consortium, JET, Culham Science Centre, Abingdon, OX14 3DB, UK*
[3]*CEA, IRFM, F-13108, St-Paul-Lez-Durance, France*
[4]*ITER Organization, Route de Vinon sur Verdon, 13067 Saint Paul Lez Durance, France*
[5]*ICREA, Pg. Lluís Companys 23, 08010 Barcelona, Spain.*
[6]*EURATOM/CCFE, Fusion Association, Culham Science Centre, Abingdon, Oxon OX14 3DB, UK*
[7]*Max Planck Institute for Plasma Physics, Boltzmannstr. 2, 85748 Garching, Germany*

## Introduction

ITER operation in its high fusion performance DT scenarios relies on the achievement of the H-mode confinement regime, which is expected to lead to the quasi-periodic triggering of ELMs (Edge Localized Modes). The energy fluxes associated with natural (or 'uncontrolled') ELMs are expected to produce excessive erosion and/or superficial surface damage on the plasma facing component and large W influxes due to sputtering during the ELMs. Controlled triggering of ELMs by the injection of small deuterium-ice pellets at frequencies significantly exceeding those of uncontrolled ELMs is one of the foreseen schemes to control ELM energy losses, divertor power fluxes and W production during ELMs. Although the technique has been demonstrated to decrease ELM energy loss successfully in ASDEX Upgrade [1], JET [2], and DIII-D [3], uncertainties still remain regarding the physics understanding as well as of the consequence of its application, such as localised power loads associated with this technique [4]. The non-linear MHD simulations with the JOREK code [5,6] have been performed to study the dependence of the pellet size required to trigger an ELM in ITER plasma, and also the dependency of the threshold on the pedestal plasma pressure when the pellet is injected; based on the assumption of that the pedestal pressure leading to spontaneous ELM triggering is 150 kPa, pedestal pressure of 75 kPa and 112.5 kPa have been studied. The work contributes the estimation of the requirement of the pellet injection condition to control ELMs in ITER 15MA operation scenarios.

## Implemented pellet modelling in JOREK

The non-linear MHD code JOREK includes a model for the density source coming from the ablation of an injected deuterium pellet [5, 6, 7]. The pellet is assumed to travel along a straight line with a given fixed velocity. The amplitude of the space and time varying density source is such that the integrated source rate is consistent with the NGS (Neutral Gas Shielding) pellet ablation model [8]. With non-linear MHD equations, the pellet ablation process is calculated self-consistently. The ablation of the pellet as it travels into the plasma causes a large local, moving density source. Since the deuterium pellet injection is mostly adiabatic, the temperature at the location of the density source will drop such that the local pressure stays constant initially. Due to the large heat conductivity, the region over which the density perturbation extends will be quickly heated up. This results in a strong local increase of the pressure which triggers an ELM.

## Pellet triggered ELM in ITER 15MA/5.3T Q=10 operation scenarios

The ITER plasma equilibrium profiles which have the pressure of 150 kPa, 112.5kPa and 75 kPa at the pedestal top are prepared as shown in Fig. 1. The distance to the edge MHD

stability limit of the target plasma is varied by changing the pedestal pressure gradient, and, self-consistently, the pedestal bootstrap current in a given number of steps (at 50% and 75% of the maximum stable condition which corresponds to the 150kPa of the pressure at the pedestal top). There will be three pellet injection ports in ITER plasma as shown in Fig. 2. In JOREK, the initial pellet locations are chosen to be located slightly outside of the separatrix.

The dependence of ELM size on the pellet size has been studied for the pedestal pressure of 75 kPa. The pellet injection velocity is 300 m/s, and the injection location is the Xpoint region. Simulations of the pellet injection from the Xpoint region have been performed with the toroidal modes n of n=0-10. The pellet size has been varied from $1.0\text{x}10^{21}$D/pellet (3.0mm of cylindrical pellet) to $4.0\text{x}10^{21}$D/pellet (4.7mm), with pellet injection speed of 300m/s; the time of injection of the pellet is t=2443.1μs. The pellet ablation rate profile versus normalized flux is shown in Fig. 2. The pellet ablation profiles show some oscillations in the vicinity of the time of the maximum pellet ablation rate. This is due to the interaction between the pellet ablated particles and the local plasma temperature. Figure 3 shows the time evolution of the magnetic energies of toroidal modes of n=8-10. The pellet triggering ELM appears at 2800μs for the largest pellet case, $4.0\text{x}10^{21}$D. The duration of the ELM crash due to the pellet triggered ELM is 600μs-800μs which is a reasonable value.

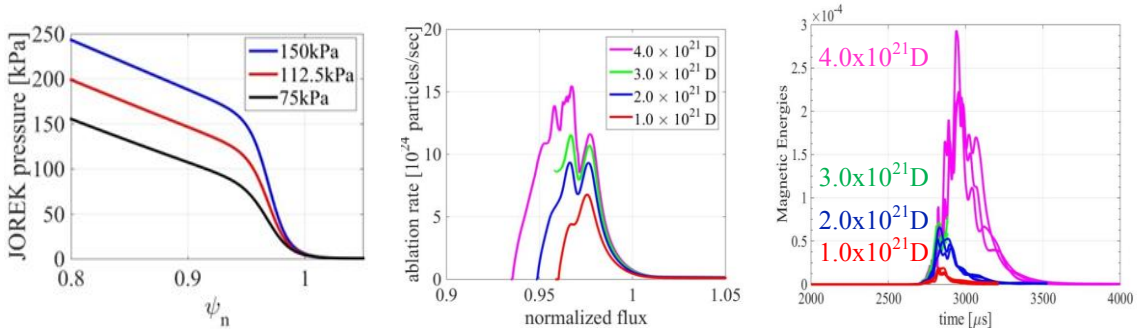


Figure 1 (left panel): The profiles of density, temperature, and the pressure for 150kPa which is unstable plasma, 112.5kPa which is in marginal of MHD stability limit, and 75kPa which is fully stable plasma. Figure 2 (middle panel): The ablation rate versus normalized flux for 4 pellet sizes. Figure 3 (right panel): The time evolution of the magnetic energies of n=8-10, for 4 pellet sizes.

Figure 4 shows the contour of the pressure perturbation on the separatrix, during the pellet triggered ELM by $4.0\text{x}10^{21}$D pellet injectio and $2.0\text{x}10^{21}$D pellet injection case at their maximum magnetic energy; t=2953μs and t=2850μs, respectively. Clear filamentary structures appear on the separatrix for $4.0\text{x}10^{21}$D not apparent for $2.0\text{x}10^{21}$D. The threshold of the pellet size to trigger an ELM is estimated between $2.0\text{x}10^{21}$D and $4.0\text{x}10^{21}$D. In order to make the estimation precise, the completion of the simulation of the pellet size $3.0\text{x}10^{21}$D is anticipated.

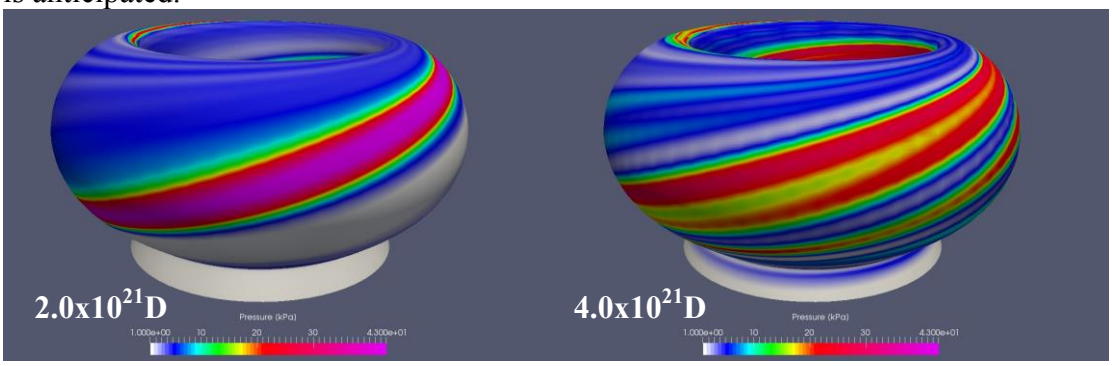


Figure 4. The contour plot of the pressure perturbation on the separatrix duing the pellet riggered ELM of 75 kPa plasma with $2.0\text{x}10^{21}$D at t=2850μs and $4.0\text{x}10^{21}$D at t=2953μs.

The pellet injections in the plasma which is in the MHD stability limit, i.e. the 112.5 kPa at the pedestal top have been carried out. The parameters of the pellet injection is identical with the studies of 75kPa. The pellet size has been varied for two sizes, $1.0x10^{21}$D/pellet and $2.0x10^{21}$D/pellet. The pellet ablation rate profile versus time and versus normalized flux is shown in Fig. 4. The 112.5kPa plasma has higher themperature profile than the one of 75kPa, therefore the pellet ablation rate is higher than the one of 75kPa case. Figure 6 shows the magnetic energies of n=8-10 after the pellet injection. The pellet $2.0x10^{21}$D increases the MHD activity strongly.

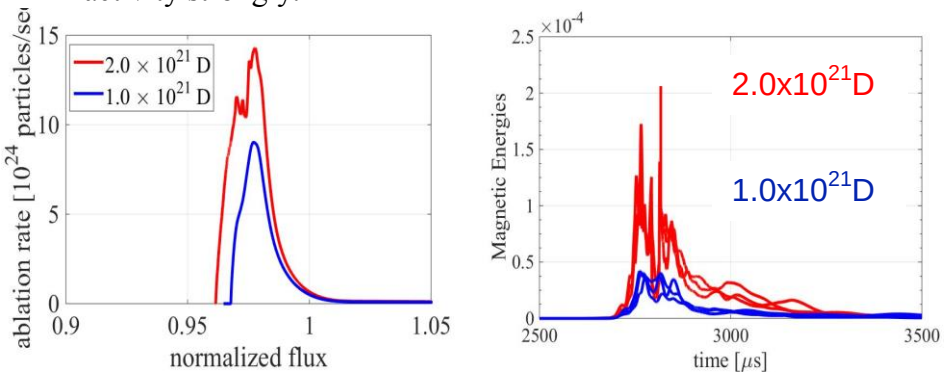


Figure 5 (left panel): The ablation rate versus normalized flux. Figure 6 (right panel): The time evolution of the magnetic energies of n=8-10.

Figure 7 shows the contour plot of the pressure perturbation on the separatrix during the pellet triggered ELM with $1.0x10^{21}$D pellet (a) and for $2.0x10^{21}$D (b) at their maximum magnetic energy; t=2721μs and t=2817μs, respectively. The scale of the colourbar is fixed for the comparison. Clear filamentary structures appear on the separatrix for $2.0x10^{21}$D pellet injection which are apparent for $1.0x10^{21}$D pellet injection case.

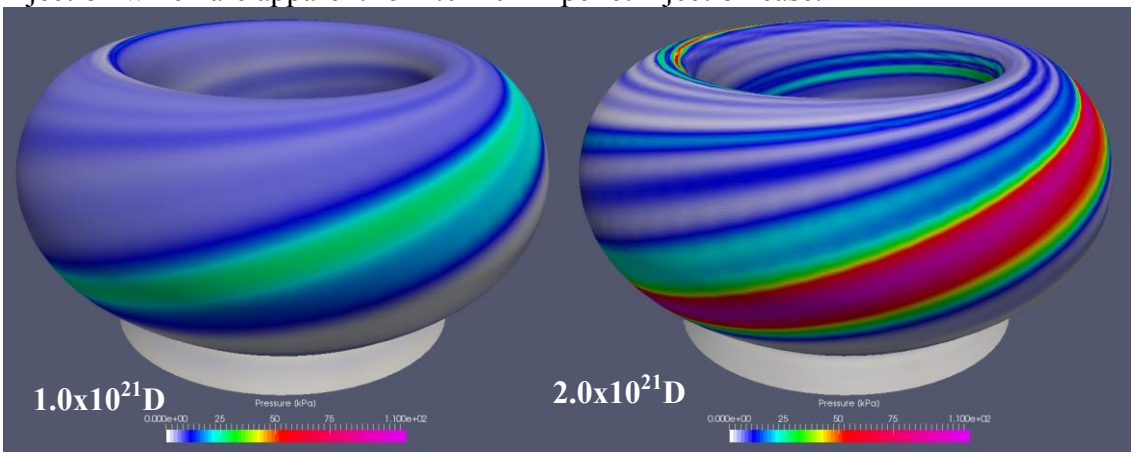


Figure 7. The contour plot of the pressure perturbation on the separatrix duing the pellet triggered ELM with $1.0x10^{21}$D pellet (a) and for $2.0x10^{21}$D (b) at their maximum magnetic energy; t=2721μs and t=2817μs, respectively.

The time evolution of the energy content inside of the separatrix is compared for 75 kPa and 112 kPa plasmas as shown in Fig. 6 and Fig. 7, respectively. The energy content in the plasma decreases due to the pellet triggered ELM. The 75 kPa shows that the energy loss has a non-linear dependence on the pellet size as shown in Fig. 6. It means the smaller pellets, such as $1.0x10^{21}$D and $2.0x10^{21}$D do not trigger an ELM while $4.0x10^{21}$D pellet triggers an ELM which leads to a large energy release from the plasma. The pellet of $1.0x10^{21}$D in 112.5 kPa plasma leads the energy loss of 0.1% of the total plasma in 100μs. The pellet injection of the

pellet size 2.0x10$^{21}$D in 75kPa plasma leads 0.23% of the total energy in 100μs while the pellet of 2.0x10$^{21}$D leads 0.47% of the energy loss in 1000μs.

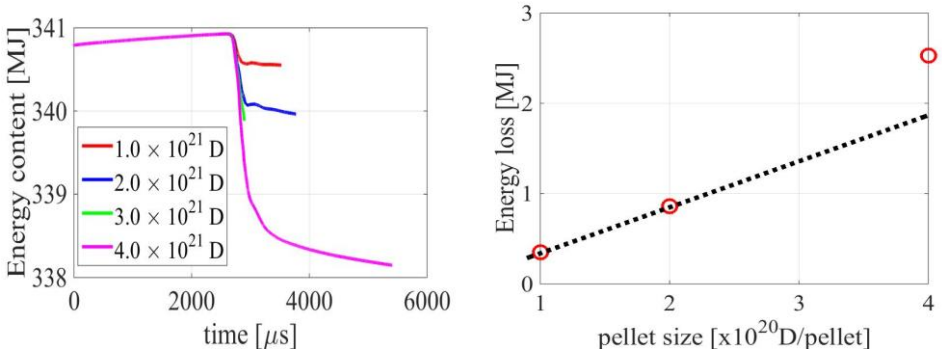


Figure 6. (left) The energy content of inside of the separatrix versus time (75 kPa plasma). (Right) The energy loss versus pellet size.

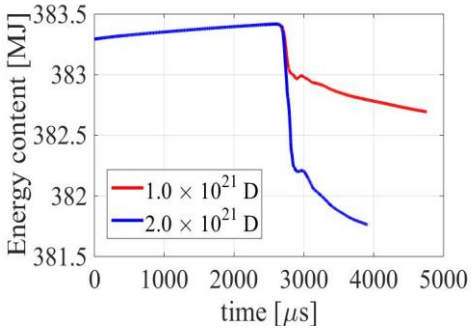


Figure 7. The energy content of inside of the separatrix versus time (112 kPa plasma).

## Conclusion

The non-linear MHD simulations with the JOREK code show that the size of the pellet required to trigger an ELM depends on the pedestal plasma pressure when the pellet is injected; for 15 MA plasmas it is necessary to increase the pellet size by a factor of 1.5 (in number of particles) to trigger ELMs for a pedestal pressure of 75 kPa compared to 112.5 kPa (note that for the pedestal assumptions in these simulations the pedestal pressure leading to spontaneous triggering of ELMs is 150 kPa). In these simulations it has also been found that the magnitude of the ELM energy loss is strongly correlated with the pedestal plasma pressure (lower at lower pressures) rather than with the size of the pellet that is required for triggering (larger at lower pressures). The next important step is to investigate the pellet triggered ELM in the presence of realistic plasma flows including diamagnetic drift, neoclassical effects, and toroidal rotation which had been neglected in previous studies.

**Acknowledgement**

This work has been carried out within the framework of the EUROfusion Consortium and has received funding from the Euratom research and training programme 2014-2018 under grant agreement No 633053. The views and opinions expressed herein do not necessarily reflect either those of the European Commission or those of the ITER Organization. The author thankfully acknowledges the computer resources of PRACE (Partnership for Advanced Computing in Europe) and RES (Spanish Supercomputing Network) at MareNostrum III and the technical support provided by Barcelona Supercomputing Center, and the support from Marconi-Fusion, the High Performance Computer at the CINECA headquarters in Bologna (Italy) for its provision of supercomputer resources.

**References**

[1] P. Lang et al., Nucl. Fusion **44** 665 (2004). [2] P. Lang et al., Nucl. Fusion **53** (2013) 073010. [3] L. Baylor et al., Phys. Rev. Lett. **110** (2013) 245001. [4] R. Wenninger et al., Plasma Phys. Control. Fusion **53** (2011) 105002. [5] G.T.A. Huysmans and O. Czarny, Nucl. Fusion **47**, 659 (2007). [6] S. Futatani et al., Nucl. Fusion **54**, 073008 (2014). [7] S. Futatani et al., 26th IAEA Fusion Energy Conference, Kyoto, Japan (2016), 43rd EPS Conference Leuven, Belgium (2016) [8] K. Gal et al., Nucl. Fusion **48**, 085005 (2008).